

# LWS spectroscopy of the luminous Blue Compact Galaxy Haro 11\*

Nils Bergvall<sup>1</sup>, Josefa Masegosa<sup>2</sup>, Göran Östlin<sup>3</sup>, and Jose Cernicharo<sup>4</sup>

1) Astronomiska observatoriet, Box 515, S-75120 Uppsala, Sweden;  
2) Instituto de Astrofísica de Andalucía, CSIC, Apdo. 3004, E-18080 Granada, Spain;  
3) Stockholm Observatory, SE-133 36 Saltsjöbaden, Sweden;  
4) Instituto de Estructura de la Materia, CSIC, Serrano 121, E-28006 Madrid, Spain

Received 0000; accepted 0000

**Abstract.** We present the results of far infrared (FIR) spectroscopy of the luminous blue compact galaxy (BCG) Haro 11 (ESO 350-IG38) obtained with the Long Wavelength Spectrometer (LWS) on the Infrared Space Observatory (ISO) in low resolution mode. This metal poor dwarf merger is an extremely hot IRAS source. We discuss the balance between dust and line cooling in the photodissociated regions (PDR), in particular the role of the [CII] $\lambda 158\mu$  line, and derive the basic properties of the PDR gas and estimates of the gas and dust masses. The mass of the PDRs,  $2_{-1}^{+2} 10^8 M_{\odot}$ , is comparable to that of the ionized gas and exceeds the observed upper limit of the HI mass. The gas/dust mass ratio is low, indicating that the galaxy contains little cold dust. The low metallicity, the intense radiation field and the low column density of Haro 11 results in an extremely high [CII]/CO flux ratio and probably also a very high  $M(H_2)/L_{CO}$  conversion factor. Therefore CO is a poor indicator of the H<sub>2</sub> mass in starburst dwarf galaxies.

After a reanalysis we confirm the claimed correlation (Malhotra et al. 1997) between the [CII] $\lambda 158\mu$ /FIR flux ratio and the IRAS  $f_{60}/f_{100}$  dust temperature and reduce the scatter. We find that Haro 11 deviates from the relationship being brighter in [CII] than what would be expected, if the mechanism proposed by Malhotra et al. is dominant. As an alternative (or complementary) explanation we propose that the [CII] $\lambda 158\mu$ /FIR versus  $f_{60}/f_{100}$  relationship is caused by an increasing optical depth with increasing IRAS temperature. The low metallicity of Haro 11 and its extreme starburst properties probably allows the medium to be thin despite its high  $f_{60}/f_{100}$  ratio. This leaves room for a more optimistic view on the possibilities to detect massive starforming mergers at high redshifts, using the [CII] line.

**Key words:** Galaxies: compact, Galaxies: evolution, Galaxies: starburst, Galaxies: ISM, Galaxies: Haro 11, Galaxies: ESO 350-IG38, Infrared: galaxies

Send offprint requests to: N. Bergvall, email:  
nils.bergvall@astro.uu.se

\* Based on observations with ISO, an ESA project with instruments funded by ESA Member States (especially the PI countries: France, Germany, the Netherlands and the United Kingdom) with the participation of ISAS and NASA.

## 1. Introduction

Blue compact galaxies (BCGs) are characterized by their high star formation rate and low chemical abundances. The high ratio between blue luminosity and HI mass,  $L_B/M_{HI}$ , combined with a high relative HI mass fraction, indicates a high star formation efficiency and a high gas consumption rate. The apparent conflict between intense star formation and low chemical abundances can only be explained if the gas containing the recently produced elements is expelled from the galaxy, if fresh gas is accreted onto the galaxy or if the galaxy is young (e.g. Searle & Sargent 1972; Makarova & Karachentsev 1998; Papaderos et al. 1998). We still have rather vague ideas about what is triggering the intense global burst. Our previous observations (Östlin et al. 1999a, 1999b) indicate that gas dynamical instabilities in connection with mergers could be the key mechanism. Under such circumstances the heating processes of the ISM could become a complicated mixture of shocks caused by infalling clouds and winds from massive young stars and on the other hand a strong radiation field from the starburst.

While optical and radio observations give us important information about the conditions in the hot ionized and the cold neutral gas in star forming galaxies we often lack information about the the ISM in the transition zone, the photodissociation regions (PDRs). The gas in PDRs contains neutral atoms and ions of low ionization potential ( $\chi < 13.6$  eV), e.g. C<sup>+</sup>. With the different possible heating mechanisms involved one would expect that the geometry and spatial extension of the ISM and the PDRs would be quite different in galaxies like Haro 11 and those with quiet star formation activity or with active nuclei, resulting in radically different spectral signatures.

Spectral diagnostics are valuable tools in dissecting the balance between different heating and cooling processes and the physical conditions in the gas. The first observations of [OI] $\lambda 63\mu$  in M82 was presented by Watson et al. (1972b). Crawford et al. (1985) for the first time showed that important information about the PDR physics in external galaxies can be obtained from the collisionally excited [CII] $\lambda 158\mu$ . Later, several studies of star forming regions in the Milky Way as well

as other starburst galaxies and ultraluminous infrared galaxies ('ULIGs', possibly hiding active nuclei) have demonstrated the power of more detailed far-IR spectroscopy (e.g. Colbert et al. 1999). An advantage with observations in the IR region is that we diminish the influence of dust extinction, allowing a more direct comparison between 'naked' starbursts in low mass galaxies and hidden starbursts in ULIGs.

The fact that  $[\text{CII}]\lambda 158\mu$  emission constitutes the peak of the flux distribution  $f_\nu$  in starforming galaxies has led to a discussion about the possibility of using  $[\text{CII}]$  to detect young galaxies at high redshifts (e.g. Petrosian et al. 1969 and the detailed discussion by Stark 1997). Despite some emerging pessimism about this possibility (Gerin & Phillips 1998) we will argue that this still is a viable idea.

As part of our multifrequency study of three of the most luminous BCGs in the southern hemisphere this report will focus on observations using the Long Wavelength Spectrometer (LWS) (Clegg et al. 1996) on the *Infrared Space Observatory* (ISO) (Kessler et al. 1996) of the luminous BCG Haro 11. Only a few emission lines in the LWS window are detectable in most nearby BCGs in a reasonably long integration time. In our case we chose to obtain clear detection of a few of these lines, with a sufficiently high S/N to allow comparisons with models and other galaxies. These lines are the  $[\text{OI}]\lambda 63\mu$ ,  $[\text{OIII}]\lambda 88\mu$  and  $[\text{CII}]\lambda 158\mu$  lines, which constitute important coolants in the far-IR regions. Among these lines,  $[\text{CII}]$  is of particular importance for reasons just mentioned and discussed below. In addition to these three lines, we obtained an upper limit on the flux in the  $[\text{OI}]\lambda 145\mu$  line in one of the adjoining detectors.

## 2. Observations and reductions

The observations were carried out during the routine observation phase of ISO in the low-resolution LWS02 observation mode with a resolution of  $0.6\mu$ . We used a scan width of 7 resolution elements, 8 samples per element and fast scanning. Each spectrum was scanned 6-111 times with a nominal 0.50 s integration time giving in total an effective integration time of 2820 s.

The data presented in this paper have been taken from pipeline 6.1. All the glitches in each individual scan have been removed by using the Interactive Analysis Software Package. About 15% of the total scans were rejected due to heavy cosmic rays contamination. In addition to the requested data the LWS spectrometer provided data on all the other detectors. These data have been also analyzed and an upper limit on the fine structure line of  $[\text{OI}]\lambda 145\mu$  has been derived. The resulting data were resampled and coadded. The data are shown in figure 1.

Except for the LWS data we also present some additional previously unpublished data in Table 1. The CO observations were carried out during June 9-12 1988 with the SEST telescope equipped with cooled Schottky receivers at 115 GHz (Jörsäter & Bergvall 1999). Six blue compact galaxies were observed and none was detected.

Optical spectroscopy was obtained with ESOs 1.5-m telescope in 1983, using the Image Dissector Scanner and an aperture of  $4''\times 4''$  arcseconds<sup>2</sup> (Bergvall & Olofsson 1986). Additional data were obtained with the IDS at the ESO 3.6-m telescope in 1986. Standard reduction techniques were used. More information is found in Bergvall & Östlin (1999a).

## 3. Results

### 3.1. General properties of the target galaxy

Haro 11 (ESO 338-IG04) is a galaxy with extreme starburst properties, summarized in Table 1. In the following we will assume a Hubble constant of  $H_0 = 65 \text{ km s}^{-1}\text{Mpc}^{-1}$ . Most of the data are from our previous observations in the UV-radio region (Bergvall & Olofsson 1986; Östlin et al 1999a, 1999b; Bergvall & Östlin 1999a and other unpublished data). Our observations show three conspicuous condensations in the centre embedded in a regular  $\text{H}\alpha$  halo. HST images (Malkan et al. 1998; Östlin et al 1999b) reveal a merger morphology. Faint wisps and indications of shell structures characteristic of galactic disk progenitors are seen in the outer regions. Our studies of the kinematics of the ionized gas indicate that the starburst is triggered by coalescing clouds involved in the merger process. The  $\text{H}\alpha$  velocity field is requires a mass of the main body of  $>10^9 \text{ M}_\odot$  (Östlin et al. 1999a; 1999b).

The oxygen abundance in the central region was calculated from the optical spectra, using the standard method. We assumed a homogeneous single metallicity model with two temperature zones. The electron temperature of the  $\text{O}^{++}$  zone was derived from the  $[\text{OIII}]\lambda 4363/([\text{OIII}]\lambda\lambda(4959+5007)$  ratio and that of the  $\text{O}^+$  zone from the semi-empirical relationship derived by Vila-Costas and Edmunds (1993). The density was derived from the  $[\text{SII}]\lambda 6717/6731$  line ratio and was found to be low. With this approach we obtain a metallicity close to 10% solar. Such a value is unusually low for a galaxy of this luminosity and deviates strongly (Bergvall et al. 1998) from the metallicity-luminosity relationship of normal dwarf galaxies (Skillman et al. 1989). Part of the optical emission may have a shock origin and we made an estimate how large the contribution from shocks may be by mixing predicted line spectra from shocked regions (Raymond 1979) with those of HII regions from Stasińska (1982). The best fits generally gave a contribution from the shock component to  $\text{H}\beta$  of  $< 5\%$ . This is in most cases not enough to change the result of the calculations of the metallicities drastically.

A surprising fact is that no HI has been detected in the galaxy (Bergvall et al. 1999b). With an upper limit of  $\mathcal{M}_{\text{HI}} = 10^8 \text{ M}_\odot$  and consequently  $\mathcal{M}_{\text{HI}}/\mathcal{L}_{B,\text{total}} < 0.01$ , it seems to be remarkably devoid of neutral hydrogen for its star formation rate. One possible explanation is that the neutral gas is ionized by the central starburst. Another possibility is that much of the gas is in molecular form. The ISO observations discussed here, which relate to the transition zone between the ionized and the cold molecular medium, will help to derive a coherent picture of the different phases of the gas.

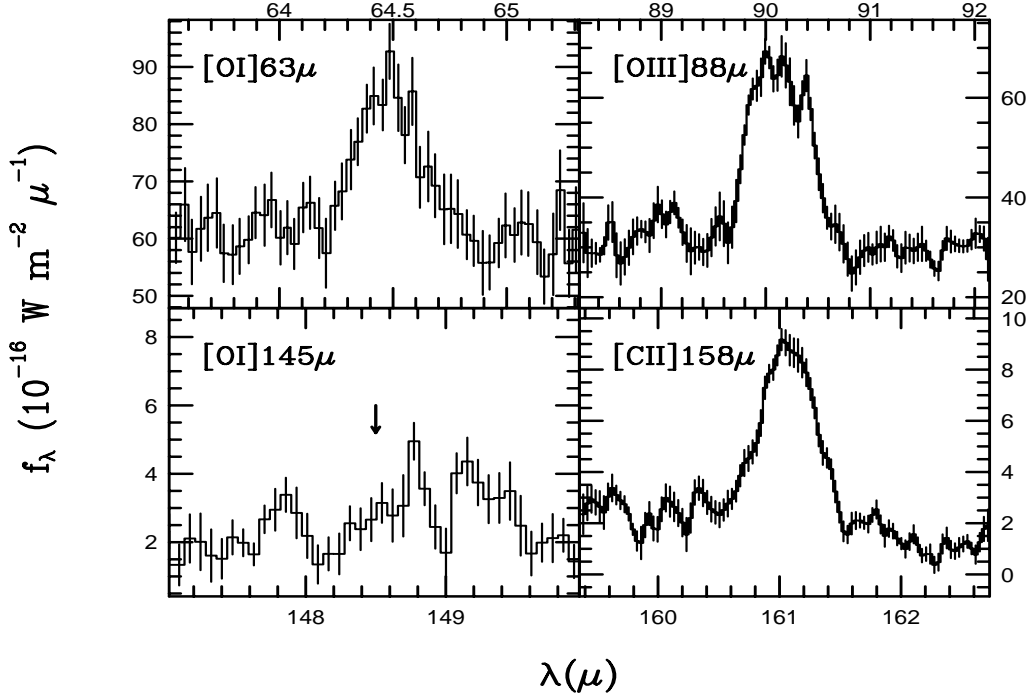


**Fig. 1.** The ISO LWS emission lines of Haro 11. 3 detections are presented. An upper limit of the flux of the  $[\text{OI}]\lambda 145\mu$  line was derived from the region at the expected position of the line, marked with an arrow. The bars indicate mean errors per pixel.

### 3.2. The dust properties

From the 60 and 100  $\mu$  IRAS fluxes and assuming a FIR grain opacity of  $\kappa = 2.5 \cdot 10^3 \lambda^{-1} \text{ cm}^2 \text{ g}^{-1}$  (Hildebrand 1983), where  $\lambda$  is the wavelength in microns, we calculate a dust temperature of  $T_{dust} = 49\text{K}$ . We can then obtain a rough estimate of the mass of the *warm* dust from (Devereux & Young 1990)

$$\mathcal{M}_{dust} = 4.58 f_{100} r^2 (e^{144/T_{dust}} - 1) \mathcal{M}_\odot$$

$f_{100}$  is in Jy and  $r$  is the distance in Mpc. We obtain  $\mathcal{M}_{dust} \sim 4 \cdot 10^6 \mathcal{M}_\odot$ .

It is interesting to compare gas-to-dust mass ratio with that of other gas rich galaxies. In Sect. 3.4.3 we find that the total hydrogen gas mass, i.e. HI, HII and H<sub>2</sub>, is approximately  $10^9 \mathcal{M}_\odot$ . We thus obtain  $\mathcal{M}_{gas}/\mathcal{M}_{dust} \sim 200$ . In a study of normal spiral galaxies, Devereux & Young (1990), taking into account only the inner part of the HI disk containing the warm dust, found that  $\mathcal{M}_{gas}/\mathcal{M}_{dust} \sim 1100$ . There is thus a difference a factor of 5-6 difference between Haro 11 and normal spirals. If the dust content correlates with metallicity, one would expect that  $\mathcal{M}_{gas}/\mathcal{M}_{dust}$  would increase with decreasing metallicity and indeed this is the case for dIrrs as was shown by Lisenfeld & Ferrara (1998). If we apply this metallicity correction in the

comparison, it would lead to an even larger difference between Haro 11 and the spirals in the  $\mathcal{M}_{gas}/\mathcal{M}_{dust}$  ratio. The high value for spiral galaxies has been shown (e.g. Chini et al. 1995) to be due to the fact that a large amount of the dust is of the cold, 'cirrus' type, radiating at longer wavelengths and thus not contributing to the mass estimates based on the IRAS data. The fact that  $\mathcal{M}_{gas}/\mathcal{M}_{dust}$  of Haro 11 is so low (in fact close to the value found for our own Galaxy, including the *total dust mass*, i.e.  $\mathcal{M}_{gas}/\mathcal{M}_{dust, total} \sim 100-150$ ) indicates that the galaxy contains very little dust at low temperature.

### 3.3. The LWS spectra

Figure 1 shows the spectral profiles of the three detected lines and the region around  $[\text{OI}]145\mu$ , for which we derived an upper limit. Table 2 summarizes the spectral data. From our optical spectra we have derived an extinction coefficient in the brightest region of the galaxy of  $A_V \approx 0.8$  mag. Thus the corrections for galactic extinction in the infrared are considerably less than the observational errors in the observed emission lines (Adams et al. 1988).

**Table 1.** General properties of Haro 11

		Ref./Note
$\alpha_{1950}$	00 <sup>h</sup> 34 <sup>m</sup> 25 <sup>s</sup> .7	
$\delta_{1950}$	-33°49'49"	
$m_B$	14.3	1/a
$v_0$	$6175 \pm 10 \text{ km s}^{-1}$	1/b
$r$	92 Mpc	3
$M_B$	-20.5	a
$a_{\mu_B=26.5}$	9 kpc	2/c
$B-V$	0.5	1/a
12+[O/H]	7.9	2
$L_{Ly\alpha}$	$9 \cdot 10^{35} \text{ W}$	3
$L_{H\alpha}$	$3.2 \cdot 10^{35} \text{ W}$	2
$L_{FIR}$	$7.4 \cdot 10^{10} L_{\odot}$	
$f_{60}/f_{100}$	1.48	
$L_{FIR}/L_B$	5.7	
$L_{CO(1-0)}$	$\leq 1.0 \cdot 10^{29} \text{ W}$	4
$\log(L_{CO}/L_{FIR})$	$\leq -8.5$	
$\mathcal{M}_{H_2}$	$\leq 10^8 \mathcal{M}_{\odot}$	d
$\mathcal{M}_{HI}$	$\leq 10^8 \mathcal{M}_{\odot}$	4
$\mathcal{M}_{HI}/L_B$	$\leq 0.01$	

a) Corrected for galactic extinction (Burstein & Heiles 1982)

b) Radial velocity, corrected to the local group according to  $v_0 = v + 300 \sin l \cos b$ , where  $v$  is the heliocentric velocity and  $l$  and  $b$  are the galactic coordinates

c)  $r$ : distance; a: major axis diameter

d) Using a conversion factor of  $3 \cdot 10^{20} \text{ cm}^{-2} (\text{K km s}^{-1})^{-1}$  (Sanders et al. 1991).

References: 1) Bergvall & Olofsson 1986, 2) Bergvall & Östlin 1999a, 3) Bergvall & Olofsson, 1999c, 4) Jörsäter & Bergvall, 1999

**Table 2.** Observed LWS data. The table shows the measured line flux, its estimated mean error and equivalent width (W) and the adjacent continuum level flux density.

Line id.	Flux ( $10^{-16} \text{ W m}^{-2}$ )	W ( $\mu$ )	Continuum flux density ( $10^{-16} \text{ W m}^{-2} \mu^{-1}$ )
[OI]63 $\mu$	$9.2 \pm 1.8$	.22	42
[OIII]88 $\mu$	$25 \pm 0.8$	.84	33
[OI]145 $\mu$	$\leq 0.3$	$\leq 0.2$	1.7
[CII]158 $\mu$	$3.9 \pm 0.1$	2.0	2.1

### 3.4. Properties of the PDR gas

One of the purposes of this study is to investigate how much the PDR gas contributes to the total mass in this type of objects, and in particular Haro 11 due to its remarkably low HI content. It is known that the relative volume of the PDR that occupies the weakly ionized (only low ionization stages) gas may be quite substantial. Regions having a total extinction of  $A_V \leq 10$  are partly photodissociated (see e.g. Crawford et al. 1985 or Tielens & Hollenbach 1985 for a general discussion

about the PDR physics). This is the situation for most of the neutral gas in the Galaxy. Estimates also show that  $\leq 40\%$  of the total gas mass in starburst nuclei are PDRs, i.e. the photodissociated gas is the dominant phase in these extreme environments (Stacey et al. 1991). The most widely used model for calculating the energy balance and obtain predictions about emissivities of the gas and dust was presented by Tielens & Hollenbach (1985). Later upgrades and applications have been discussed by Hollenbach et al. (1991), Wolfire et al. (1990) and Kaufman et al. (1999).

The Kaufman et al. standard model is based on an oxygen abundance of 40% solar, close to the local Galactic value and a factor of 4-5 higher than in Haro 11. From our derived carbon abundance in ESO 338-IG04 (Tol 1924-416), a galaxy quite similar to Haro 11, we may assume that  $N(C)/N(O) \approx 0.2$  (Bergvall 1985). Similar values have been obtained for other metal poor galaxies (Garnett et al. 1995). Thus, oxygen and carbon are underabundant with factors 4-8 with respect to the standard setup in Kaufmans et al. models (their models have  $N(C)/N(O) \approx 0.5$ ). The predicted temperature of the surface gas layers obtained from their basic diagnostic diagrams is therefore probably somewhat overestimated while still the line intensities are reasonably correct (Wolfire et al. 1990). However, Kaufman et al. also discuss a case of lower metallicity, about 4% solar and present diagrams showing how [CII], FIR and CO luminosities relate to density,  $n$ , incident far UV radiation intensity,  $G_0$ , and the two metallicities  $\approx 4$  and 40% solar. In the following we use these models to estimate some fundamental parameters of the PDR regions.

#### 3.4.1. Optical thickness

To enable a comparison of the line intensities with the models of Kaufman et al., we first estimate the contribution from HII regions to the line intensities and also the optical depth of the lines. The optical emission lines (Bergvall & Olofsson 1986 and newer data) have been used together with recent photoionization models (Stasińska 1990, and updates) to estimate the contribution to the far-IR lines from the HII regions. We used our observed line intensities in [OI], [OII], [OIII], [NII], [SII], HeI and HeII, corrected for extinction, underlying absorption and shock contribution to select the best fitting HII region models from Stasińska's library. As a result we find that the measured intensity of the [OIII] $\lambda 88\mu$  line is fully consistent with photoionization by a cluster of stars with  $T_{eff}$  of the order of 35000-40000 K. For the other 3 lines observed with the LWS, the contribution from HII regions to the measured intensity is strongest in [CII] but is still  $\leq 20\%$ . Thus, when discussing the [CII] line flux and flux ratios, we can directly compare to the predictions from Kaufman et al..

In a study of two star forming complexes in the Large Magellanic Cloud, Israel et al. (1996) concluded that these regions were optically thin at a *minimum* column density of  $3 \cdot 10^{21} \text{ cm}^{-2}$ . Since these cloud aggregates probably have similar properties as Haro 11 we can conclude that the star forming regions in Haro 11 on a local scale probably are optically thin

in  $158\mu$ . The optical extinction derived from the  $H\alpha/H\beta$ -ratio in Haro 11 is only  $A_V = 0.8$  so we don't expect that the [CII] line is optically thick even on a global scale. But the derived extinction depends on the spatial distribution of the HII regions so to assure that we don't have conditions that allow hidden sources in the central area we will estimate the optical depth in [CII],  $\tau_{[CII]}$ . This calculation will also be used to make estimates of optical depths of the other galaxies involved in the discussion.

In the high-temperature ( $T \gg 92\text{K}$ , the excitation potential for [CII]), high-density limit ( $n \gg 4 \cdot 10^3 \text{ cm}^{-3}$ , the limit for collisional deexcitation by H and H<sub>2</sub>),  $\tau_{[CII]}$  can be expressed as (Crawford et al. 1985)

$$\tau_{[CII]} = 2.3 \cdot 10^{-16} \frac{N_{C^+}}{T_{C^+} \sigma_v}$$

where  $N_{C^+}$  is the column density of C<sup>+</sup> in  $\text{cm}^{-2}$ ,  $T_{C^+}$  is the temperature of the gas in K and  $\sigma_v$  is the velocity dispersion in  $\text{km s}^{-1}$ . If we as a first rough approximation assume that the global distribution of the gas is close to a homogeneous exponential disk we can derive the central column density in atoms  $\text{cm}^{-2}$

$$N_{\text{gas}} = 1.3 \cdot 10^{14} \frac{\mathcal{M}_{\text{gas}}}{2\pi h_{\text{gas}}^2}$$

where  $\mathcal{M}_{\text{gas}}$  is the mass of the gas in solar masses and  $h_{\text{gas}}$  is the scale length in kpc. As a first approximation we will assume  $h_{C^+} = h_{H\alpha}$ . From our  $H\alpha$  images we derive  $h_{H\alpha} \sim 2'' = 1 \text{ kpc}$ . As an estimate of the gas mass we will use our upper observational limit of  $\mathcal{M}_{HI}$ , i.e. around  $10^8 \mathcal{M}_\odot$ . With this we obtain a central column density in HI of  $N_{HI} \sim 2 \cdot 10^{21} \text{ atoms cm}^{-2}$ . Later we will find it consistent to assume that most of the HI actually is associated with the PDR regions. Part of the C<sup>+</sup> region in the PDR also contains molecular gas. In sect. 3.4.2 we will show that this may increase the estimated column density with a factor of 2.

The C<sup>+</sup> column density can now be derived from

$$N_{C^+} \approx 1.3 \cdot 10^{14} X(C^+) \frac{\mathcal{M}_{HI}}{2\pi h_{H\alpha}^2}$$

where  $X(C^+)$  is the relative abundance of carbon ions to hydrogen atoms. With these approximation we can write the optical depth as

$$\tau_{[CII]} \leq 0.03 X(C^+) \frac{\mathcal{M}_{HI}}{T_{C^+} \sigma_v 2\pi h_{H\alpha}^2}$$

Since most of the carbon in the [CII] emitting region is in ionized form we will assume  $X(C^+) \approx X(C_{\text{total}}) \approx \frac{N(C)}{N(O)} X(O) \approx 1.2 \cdot 10^{-5}$ . In starburst galaxies  $T_{C^+}$  is typically a few hundred K. We will later iteratively derive  $T_{C^+}$  and obtain a value below 400K. From our Fabry-Perot observations in  $H\alpha$  of the central region we estimate  $\sigma_v \sim 60 \text{ km s}^{-1}$ . We then obtain  $\tau_{[CII]} \leq 0.001$ . In order to derive a more realistic estimate, we have to take into account that the gas has a lumpy, fractal distribution. But it is sufficient to note that, assuming a volume

filling factor  $\alpha$  of a few per mille (Crawford et al. 1985), the surface density would increase with  $\sim \alpha^{-2/3}$ , i.e. a few tens. Thus it still would be safe to assume that the medium is thin in [CII]. The optically thick limit at a chemical abundance similar to Haro 11 would be at a mean column density of  $N_{HI} \sim 10^{23} \text{ atoms cm}^{-2}$  and with solar abundances  $N_{HI} \sim 10^{22} \text{ atoms cm}^{-2}$ , still with the assumption that the filling factor is a few per mille.

### 3.4.2. The mass of the PDR gas

From the diagnostic diagrams by Kaufman et al. we can obtain the density and intensity of the incident far-UV flux  $G_0$  in the PDR region. We use two diagrams for this purpose, one utilizing the [OI]63μ/[CII]158μ intensity ratio and one utilizing the ([OI]63μ+[CII]158μ)/FIR ratio. As mentioned above, before we use the predictions we need to correct for the difference in metallicity between Haro 11 and the models, a factor of 3-4. We can estimate what effect this may have by comparing the predicted fluxes of these lines in an HII region at the different metallicities. The column densities and thus the volume emissivities of the low ionization lines are lower in HII regions than in a typical PDR region but the flux ratios should vary in approximately the same way. From Stasińska's models we find that the difference in flux ratios, assuming a constant N(C)/N(O), is about 2 %. N(C)/N(O) probably differ with a factor of about 2 however, and so we should make an appropriate correction for this which means a factor of 1.5-2 in the [OI]63μ/[CII]158μ ratio. Kaufman et al. show in later diagrams that the metallicity has a minor effect on the [CII]158μ/FIR ratio in the region of the parameter space where we are residing.

We now feel confident to compare the slightly corrected line intensities with the predictions from the PDR models. Using the [OI]63μ, [CII]158μ line fluxes and the FIR flux, Kaufman et al. diagnostic diagrams show that  $G_0$  is  $1-2 \cdot 10^3$  in units of the Galactic far-UV field ( $1.6 \cdot 10^{-6} \text{ W m}^{-2}$ ). The obtained value for the density is  $n \approx 2 \cdot 10^3 \text{ cm}^{-3}$  and thus  $G_0/n \approx 1-2 \text{ cm}^3$ . These are typical values for normal starforming regions and galaxies (Tielens & Hollenbach, 1985; Wolfire et al. 1990; Carral et al. 1994; Fischer et al. 1996). The surface temperature is  $T \sim 400\text{K}$ . The data are summarized in Table 3. With these data at hand we can obtain the predicted [OI]145μ/[OI]63μ ratio which is approximately 0.06. This is within the errors of the measured line ratio and thus supports the reliability of the model.

From the measured [CII] flux we may now calculate the mass of the warm atomic gas according to (e.g. Wolfire et al. 1990)

$$\mathcal{M}_{\text{PDR}} = 5.96 \cdot 10^{15} \frac{r^2 f_{[CII]} m_H}{\Lambda(CII) X(C^+)} \mathcal{M}_\odot$$

where  $r$  is the distance to the galaxy in Mpc,  $f_{[CII]}$  is the [CII] flux in  $\text{W m}^{-2}$ ,  $m_H$  is the mass of the hydrogen atom in kg, and  $\Lambda(CII)$  is the cooling rate per atom in the 158μ line in W. In the high-temperature and high-density limit  $\Lambda(CII)$  will be nearly independent of the temperature (Wolfire et al. 1990).

$\Lambda(\text{CII})$  can therefore be rather safely estimated and we obtain  $\Lambda(\text{CII}) \approx 1.3 \cdot 10^{-26} \text{ W atom}^{-1}$ . In the surface layers of the PDR carbon is mainly in the low ionization monoatomic state so  $\text{X}(\text{C}^+) \approx \text{X}(\text{C})$ . We then derive  $\mathcal{M}_{\text{PDR}} \approx 2_{-1}^{+2} \cdot 10^8 \mathcal{M}_\odot$ .

### 3.4.3. The mass fractions of cold, warm and ionized gas

The value we have derived for the mass of the PDR:s is larger than or comparable to our upper limit of the HI mass, i.e.  $10^8 \mathcal{M}_\odot$ , indicating that most of the HI gas is located in the PDR regions if these are dominated by the atomic gas component. The total molecular gas mass in normal star forming regions is normally 5-10 times larger than in the PDR regions. Data from other starburst galaxies however indicate that considerably lower values are more likely (e.g. Wolfire et al. 1990; Stacey et al. 1991). This is probably a metallicity effect. In galaxies with low metallicities the UV radiation can penetrate deeper into the molecular clouds, increasing the PDR zone relative to the CO core. An upper limit is therefore probably around  $10^9 \mathcal{M}_\odot$  in our case. This mass estimate may be compared to the upper limit of the  $\text{H}_2$  mass, derived from the CO (1-0) observations which is  $\leq 10^8 \mathcal{M}_\odot$ . The calculation of this last value is however rather uncertain due to the uncertainty in the conversion factor between the CO flux and  $\mathcal{M}_{\text{H}_2}$  (Maloney & Black 1988, Taylor et al 1998). As just mentioned, the low metallicity also allows a larger proportion of  $\text{H}_2$  to be hidden in the CO dissociated zone. Therefore, in addition to the problem caused by the uncertainty in the conversion factor between CO and  $\text{H}_2$ , the CO fluxes are poor indicators of the  $\text{H}_2$  masses in low metallicity galaxies.

Using the available photometry of the halo and the burst, our spectral evolutionary models predict a total stellar mass of  $1.5 \cdot 10^{10} \mathcal{M}_\odot$ , while the observed rotation results in a mass of  $\sim 2 \cdot 10^9 \mathcal{M}_\odot$ , assuming dynamical equilibrium (Östlin et al. 1999a; 1999b). The discrepancy between the photometric and dynamical mass estimates can be resolved if the galaxy is dominated by velocity dispersion, which is reasonable if the width of the  $\text{H}\alpha$  line reflects potential motions, or if the galaxy is not in dynamical equilibrium.

From the global  $\text{H}\alpha$  luminosity and the mean density of the gas, derived from our spectra, the mass of the ionized gas is estimated to be  $\sim 10^8 - 10^9 \mathcal{M}_\odot$  (Östlin et al. 1999a, 1999b). It is a remarkable fact that the HI mass is so low and also lower than or comparable to the estimated mass of ionized or molecular gas. A possible explanation may be that HI to a large extent has become molecular and/or ionized in the merging process. If this is correct, then the gas/total mass estimates may have been severely underestimated in many dwarf starburst cases. This will complicate the efforts to understand dwarf galaxy evolution in general. A summary of the mass estimates is found in Table 4.

### 3.5. Thermal balance and the $[\text{CII}]/\text{FIR}$ ratio

The important coolant  $[\text{CII}]\lambda 158\mu$  originates from the surface layers of PDRs where the  $\text{C}^+$  ions are excited by photoelec-

**Table 3.** Global data, based on the LWS observations

$G_0$	$1\text{-}2 \cdot 10^3$
$n$	$2 \cdot 10^3 \text{ cm}^{-3}$
$G_0/n$	$\approx 1 \text{ cm}^3$
$T$	$< 500 \text{ K}$
$L_{[\text{CII}]\lambda 158\mu}/L_{\text{CO}}$	$\geq 4 \cdot 10^5$
$L_{[\text{CII}]\lambda 158\mu}/L_{\text{FIR}}$	$1.4 \cdot 10^{-3}$
$(L_{[\text{OI}]\lambda 63\mu} + L_{[\text{CII}]\lambda 158\mu})/\text{FIR}$	$4.6 \cdot 10^{-3}$
$L_{[\text{OI}]\lambda 145\mu}/L_{[\text{OI}]\lambda 63\mu}$	$\leq .03$
$L_{[\text{OI}]\lambda 158\mu}/L_{[\text{OI}]\lambda 63\mu}$	0.42

**Table 4.** Mass estimates ( $\mathcal{M}_\odot$ )

HI	$\leq 10^8$
HII	$10^8\text{-}10^9$
$\text{H}_2$	$10^8\text{-}10^9$
PDR	$2_{-1}^{+2} \cdot 10^8$
Warm dust	$4_{-2}^{+4} \cdot 10^6$
Photometric	$1.5_{-0.5}^{+2} \cdot 10^{10}$
Rotational <sup>1</sup>	$2_{-1}^{+8} \cdot 10^9$

1) Assuming dynamical equilibrium

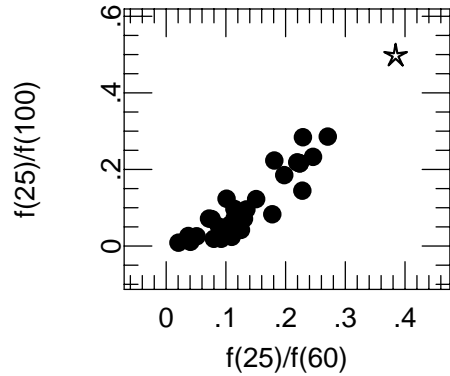


**Fig. 2.** The IRAS  $f_{25}/f_{60}$  versus the  $f_{25}/f_{100}$  micron flux ratios for Haro 11 (star) and the comparison sample (filled dots)

trons ejected from grains heated by the UV radiation (Watson 1972a). PAHs are believed to be the dominating agent of this process. Stacey et al. (1991) studied a mixed sample of spiral galaxies, starburst galaxies, giant molecular clouds and galactic star forming regions and noticed that while there is a linear relation between the energy density of the UV field and the cooling rate of the dust, the efficiency with which the [CII] line is excited seems to decrease with the intensity of the UV field. One should have in mind however that this is not a homogeneous sample. Malhotra et al. (1997) investigated the same relationship between the [CII] cooling and dust cooling for dif-

ferent types of galaxies, using the [CII]/FIR luminosity ratio. An anticorrelation was found between the [CII]/FIR ratio and dust temperature, as measured by the IRAS  $f_{60}/f_{100}$  ratio. After a discussion of several possible explanations, Malhotra et al. found it most probable that this is a consequence of a decreasing efficiency of ejection of photoelectrons from the grains, reducing the [CII] intensity. Theoretically it can be understood if the ratio of UV flux to gas density, and thus the dust temperature, becomes high because the dust grains would be more positively charged, forming a stronger Coulomb barrier against photoejection.

One should be aware, both as regards the results from Malhotra et al. and in the following discussion, that the sample for which useful data are available is quite heterogeneous. The galaxy types involved range from normal galaxies to Seyferts for which the relative importance of different heating sources (stars and AGNs) and different chemical abundances are not satisfactorily controlled. Moreover, in the first approximation, two dust components, warm and cold, having different spatial distribution, can be separated. This increases the complexity in the interpretation of the global data and the 60/100 index as well as the  $L_{FIR}/L_B$  index cannot be regarded as clearcut tracers of the star formation activity. As a consequence we expect that the scatter in the discovered trends will remain quite large.

We will now compare the data for Haro 11 with a data set similar to that used by Malhotra et al. but including more detected galaxies at relatively high  $f_{60}/f_{100}$ . These data were obtained from Stacey et al. (1991), Luhman et al. (1998), Malhotra et al. (1997) and Lord et al. (1996).

For the most nearby galaxies, having velocities  $\leq 500$   $\text{km s}^{-1}$ , we have scanned the literature to find the most recent distance determinations derived from photometric distance indicators. This concerns the galaxies M82, NGC 3109 (Kennicutt et al. 1998), NGC 4414 (Turner et al. 1998), NGC 4736 (Garman & Young 1986), NGC 5128 (Tonry et al. 1995), NGC 5194 (Sandage 1987), NGC 6946 (Freedman et al. 1994) and IC 342 (Krismer et al. 1995). In order to take proper account of the mid-IR contribution to the FIR luminosities, the FIR luminosities were calculated from  $\text{FIR} = 5.35 \cdot 10^5 r^2 (12.66 f_{12} + 5.00 f_{25} + 2.55 f_{60} + 1.01 f_{100}) L_\odot$ , where  $r$  is the distance to the galaxies in Mpc and  $f_{12}$ ,  $f_{25}$ ,  $f_{60}$  and  $f_{100}$  are the apparent flux densities in Jy (Belfort et al. 1987), instead of the normal approximation, e.g.  $\text{FIR} = 3.75 \cdot 10^5 r^2 (2.58 f_{60} + 1.0 f_{100}) L_\odot$  (Lonsdale & Helou 1985). This choice makes a small but noticeable change in the distribution of the data in the diagrams.

Fig 2 displays the distribution of Haro 11 and the comparison sample in the IRAS  $f_{25}/f_{60}$  vs.  $f_{25}/f_{100}$  diagram, showing the extreme position of Haro 11. Fig. 3 shows the FIR/B-60/100 diagram for the sample galaxies. In the diagram are also indicated the loci of normal spiral galaxies and blue compact galaxies (Dultzin et al. 1988). As we see, Haro 11 also in this case lies at the extreme of the BCG distribution. The extremely strong  $25\mu$  emission confirms the lack of cold dust and indicates the presence of a strong nuclear starburst (Dultzin-Hacyan et al. 1988; Hawarden et al. 1986; see also Boulanger

et al. 1994; Taniguchi et al. 1990), destroying the smallest dust grains (e.g. Desert 1990).

Fig. 4 and 5 correspond to Malhotras et al. diagram 1. To extract the most important global parameters involved in the relation reflected in fig. 4, we made a cross correlation test between the [CII]/FIR flux ratio, the IRAS data (i.e. the ratios between the 12, 25, 60 and  $100\mu$  fluxes), the FIR/B flux ratios and the FIR flux. We found strong correlations ( $\geq 6\sigma$ ) between only three of these parameters:  $f_{60}/f_{100}$ , FIR/B and the [CII]/FIR ratio.

In figure 4 the trend found by Malhotra et al. is confirmed and appears even stronger. But it is also evident that the position of Haro 11 deviates from the envelope defined by the other galaxies. The possible explanations for the deviant position of Haro 11 are either that there is an excess in the [CII] over FIR luminosity or that the  $f_{60}/f_{100}$  temperature is high, or both. Let us look at these two options one at a time. A consequence of lower metallicity is that the UV photons penetrate deeper into the cloud, thus increasing the volume of the PDR region at the expense of the colder molecular core. Strong observational support of this in terms of a high [CII]/CO flux ratio have been reported by e.g. Mochizuki et al. (1994), Poglitsch et al. (1995), Madden et al. (1997), Smith & Madden (1997) and Israel et al. (1996). Haro 11 behaves in the same way with its extremely high [CII]/CO ratio ( $> 4 \cdot 10^5$ ). The interesting question is how much the [CII]/FIR ratio will be influenced by varying metallicity under these conditions. The models by Kaufman et al. show that [CII]/FIR is almost unaffected by metallicity variations in cases where  $G_0/n$  have normal values. This is also in agreement with observations. In 30 Dor and the cases discussed by Israel et al. however, the  $G_0/n$  ratio is low ( $\leq 0.1$ ) which results in a diluted radiation field, an increased heating efficiency and brighter [CII] emission. In Haro 11 the  $G_0/n$  ratio is normal ( $G_0/n = 1 \text{ cm}^3$ ), as seen from table 3. So, both observations and modelling argue against an increase in [CII]/FIR in Haro 11 due to low metallicity. There is also another reason. In fig. 5 Haro 11 adheres to the other galaxies in the diagram. Therefore as a first guess it is reasonable to assume that [CII]/FIR is normal while  $f_{60}/f_{100}$  is deviating.

We concluded in section 3.2 that Haro 11 contains very little warm or cold dust. Haro 11 is a merging system of galaxies and it is possible that the merging galaxies have lost their cold dust components, e.g. extended disks, in the merger process. Is it possible that the lack of a 'normal' cold dust component could explain the high  $f_{60}/f_{100}$  ratio? Would the contribution from such a component be sufficient to move the position of Haro 11 into the region of the other galaxies? It is an important question to ask since it separates global phenomena from local ones. We have made a rough check of this possibility by selecting the galaxies in the comparison sample having apparent sizes sufficiently large to allow us to obtain IRAS data both from the very centre and also the integrated IRAS fluxes of the entire galaxy. In this way we can have an idea about how much the extended component influences the 60/100 ratio. It turns out that in the majority of the cases the IRAS temperature actually *increases* when the extended component is included.

Moreover, for the hottest cases, the hot component is always significantly stronger than the warm/cold component, if existing. Our impression is therefore that the IRAS temperature of the warm dust of the most active regions in Haro 11 and the galaxies below Haro 11 in fig. 4 are similar.

Although we expect a large scatter in fig. 4 we should examine if there may be other parameters involved ruling the balance between [CII] and FIR emission and explaining part of the scatter in the diagram and the deviant position of Haro 11. Since both the spectrum of the radiation field and the spatial distribution of gas and dust in general differs between low-mass starbursts and galaxies with AGNs, we could suspect that we would also find systematic differences in the [CII]/FIR ratios between these types of galaxies. When comparing galaxies classified in the optical region as Sy1, Sy2, liners and HII galaxies we find that the HII galaxies appear to have a broad distribution in  $f_{60}/f_{100}$  while the Sy2 and liners tend to concentrate towards high IRAS temperatures and high FIR/B. Similarly, in a statistical investigation of the IR/optical properties of BCGs as related to Seyfert and Liner galaxies (Dultzin-Hacyan et al. 1988, 1990) it was shown that the  $f_{25}/f_{100}$  is a powerful index that can be used to discriminate between pure starbursts and cases where AGNs are important for the radiation field.

### 3.6. What rules the [CII]/FIR ratio?

Several possible physical mechanisms have been proposed to explain the trends in [CII]/FIR seen in fig. 4 and 5 (e.g. Malhotra et al. 1997; Luhman et al. 1998). As we already mentioned, Malhotra et al. argued that the reduced efficiency in photoejection due to a hard radiation field could be a plausible explanation. The data for Haro 11 however, acts as a counterexample of this. Both optical spectroscopy and the 'hot' IRAS indices indicate a hard radiation field. Still, the [CII]/FIR is close to the values of normal, more passive galaxies. An alternative explanation, that have been discussed by Malhotra et al. and others is that [CII] actually is optically thick in many of the cases where the [CII]/FIR ratio is low. The general opinion seems to be that the [CII] line is optically thin. These conclusions are based on estimates of the optical depth in a few well known cases, e.g. M82 (Crawford 1985). But M82 is behaving well in the diagrams (see fig. 5) and the central column density of the gas is not abnormal. From the discussion above we see that, depending on the velocity field and the relative amount of molecular gas in the C+ zone, the medium could become optically thick in [CII] at a column density of  $N \sim 10^{22-23} \text{ cm}^{-2}$ . Such high numbers can be found in the central regions of some luminous starburst galaxies. Gerin & Phillips (1998) elaborated on the low [CII]/FIR ratio in Arp 220 and it is interesting to compare this galaxy with M82 and Haro 11 (see fig. 5). They came to the conclusion that with an estimated column density of  $N \sim 10^{24} \text{ cm}^{-2}$ , the *dust opacity and emission* would be sufficiently high to explain at least part of the low value of [CII]/FIR. But in fact there may be three sources responsible for reducing the ratio: dust opacity, dust emission and self absorption. What is maybe most important is how to explain why the [CII]/ $L_{Bol}$  ra-

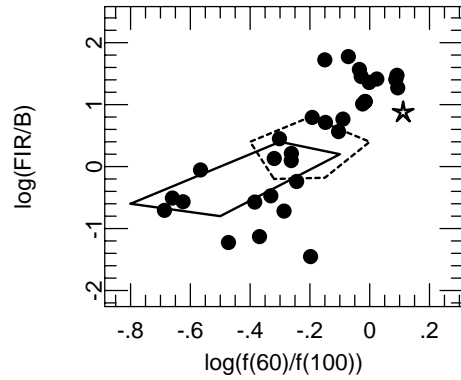


**Fig. 3.** The FIR/B luminosity ratio vs. the IRAS temperature  $f_{60}/f_{100}$  for the same sample as in fig. 2. The full drawn box indicates the locus of normal spiral galaxies and the hatched box the locus of blue compact galaxies according to Dultzin et al. 1988

tio decreases with FIR/B. Therefore the combined effect of dust absorption and [CII] selfabsorption should be investigated.

Fig. 6 shows the same data as in fig. 5, divided into different galaxy types, Sy1, Sy2, HII and Liners. As we can see, there is a predominance of Sy2 galaxies and Liners at high FIR/B. Most of these galaxies are ULIGs. There are strong indications that Liners are galaxies with massive nuclear starbursts and likewise some of the Sy2 galaxies. Many of these galaxies are probably remnants of massive merges. Even though the luminosity of some of them are not extreme, high column densities could possibly be obtained also in less massive nuclear starbursts, provided they are sufficiently compact. Such very compact nuclear starbursts are preferentially found in the type of galaxy we find at high FIR/B in the diagram (Heisler & Vader 1986). In a simplified form fig. 6 shows the effect of increasing optical depth on the sample. Where the gas is optically thick in [CII] the ratio between the [CII]/B flux ratio should be approximately constant. Where it is thin, [CII]/FIR should be constant.

### 4. [CII] as a probe of high redshift starbursts

As we can see from figure 4 and 5, the [CII] line in starburst galaxies has a maximum luminosity of a few per mille of the bolometric luminosity and constitutes the peak in the spectral distribution from radio to X-ray. It has therefore been proposed (e.g. Petrosian et al. 1969; Loeb 1993; Stark 1997) that it can be used as a probe in searches for high redshift starburst galaxies. At redshifts of  $z \geq 5-6$ , where current models of galaxy formation predict the first massive galaxies to form and where optical-near IR observations start to reach the confusion limit, the [CII] line is shifted into the submillimeter (submm) region and could be detected with a suitable submm telescope at a cold

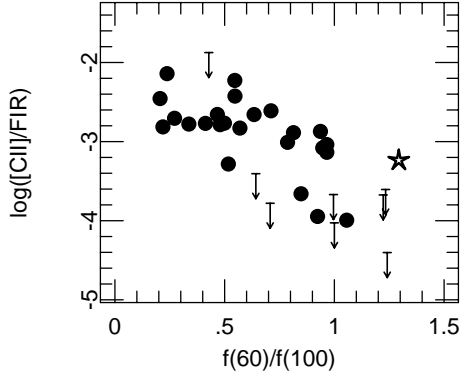


**Fig. 4.** The [CII]/FIR ratio vs. the IRAS temperature  $f_{60}/f_{100}$  for the same sample as in fig. 2. Upper limits are marked with arrows.

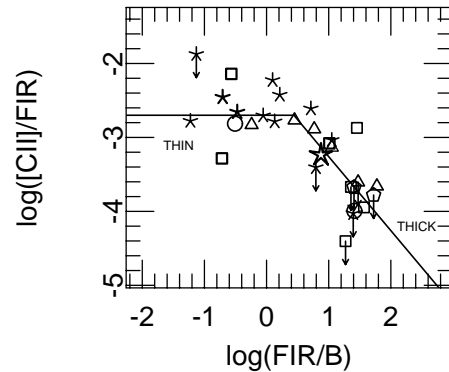


**Fig. 6.** The [CII]/FIR ratio vs. the FIR/B luminosity ratio as in fig. 5. Upper limits are marked with arrows. The different activity classes have been coded according to: Circle-Sy1, Square-Sy2, Triangle: Liner, Star: HII, Pentagon: Unclassified. The full drawn line shows an idealized approximation of the effect of increasing optical depth with FIR/B.

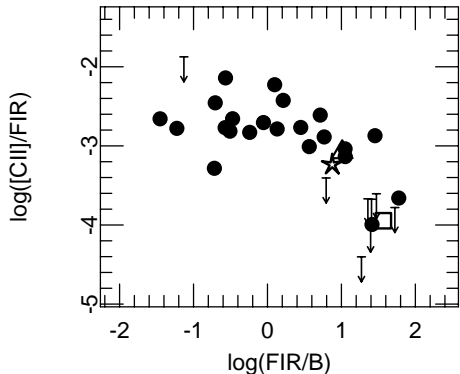


**Fig. 5.** The [CII]/FIR vs. the FIR/B luminosity ratios for the same sample as in fig. 2. M82 is marked with a triangle and Arp220 with a square. Upper limits are marked with arrows.

dry site like the South Pole (Stark 1997). The most interesting targets would probably be massive starburst mergers, characterized by a high 60/100 ratio and a high FIR/B ratio. The tendencies seen in the study of Malhotra et al. (1997) however, have created some pessimism (e.g. Gerin & Phillips 1998) about the feasibility, due to the rapid decrease in the relative strength of the [CII] line with IRAS temperature. The properties of Haro 11 however, indicate that the conditions may be more promising than anticipated since the [CII]/ $L_{Bol}$  of this galaxy is close to the value obtained for the normal galaxies. If this is due to the low metallicity of the galaxy or not remains to be explored but if so it may apply on distant metal-poor galaxies. The detection probabilities derived by Stark (1997) predict that it would be quite possible to detect a galaxy with a mass equal to that of

a present day  $L^*$  galaxy at  $z=4-5$  in a few hours, using a 10m submm telescope at the South Pole. At the formation epoch a massive galaxy would be several magnitudes brighter than today, i.e.  $\sim 10^{12} L_\odot$ . Thus we would need to merge about 10 Haro 11 type galaxies to produce this luminosity. A beam size of  $20''-30''$  for a 10m telescope corresponds to about 100 kpc at the redshift we discuss. Thus it would easily encompass a compact merging group of dwarf galaxies and make a detection feasible. Moreover, with the advent of planned large sub-mm/mm arrays (e.g. ALMA), the prospects for using the [CII]158 line as a probe of high redshift starburst would be even more interesting.

## 5. Conclusions

We have reported about ISO LWS observations of the luminous metal poor BCG Haro 11 in the three prominent emission lines [OI]63 $\mu$ , [OIII]88 $\mu$  and [CII]1588 $\mu$ . The galaxy is involved in an intense global starburst probably due to a merger of dwarf galaxies. The ISO data and previous observations in the optical-radio region in combination with model predictions are used to derive information about the physical properties of gas and dust in the galaxy.

Haro 11 is one of the hottest IRAS galaxies observed and we find no trace of cold dust. Most of the neutral hydrogen is confined to the photodissociation regions. The main part of the gas however, appears to be in ionized or molecular state. This possibility is generally neglected when discussing the gas content in starburst dwarfs, leading to serious underestimates of the total gas mass.

We also reinvestigate the claimed correlation between [CII] emission, far-IR luminosity and the IRAS 60/100 temperature

for a number of starforming galaxies of different types, active and non-active. We confirm and tighten the correlation and note that Haro 11 deviates in the sense that its  $[\text{CII}]/L_{\text{FIR}}$  is higher than expected. We argue that this may indicate that the previously preferred explanation of the relationship, a decreasing efficiency with IRAS temperature in the ejection of photoelectrons from UV-illuminated grains may not be entirely correct. An alternative, or complementary explanation seems to be that the optical depth increases with increasing IRAS temperature. This would be expected if the IRAS temperature correlates with compactness and/or mass of the central starburst region. The metallicity may also play an important role, in which case the somewhat pessimistic opinions about using  $[\text{CII}]158\mu\text{m}$  to detect high redshift massive starburst galaxies may not be valid. The whole situation will probably be clarified once a more representative sample of galaxies, including both normal dwarfs and massive galaxies becomes available.

**Acknowledgements.** We gratefully acknowledge partial support from the Swedish Natural Science Research Council and the Swedish Space Board. JM and JC are supported by Spanish CICYT grant ESP98-1351. JM has been also supported by DIGCYT grant PB93-0139. G. Östlin acknowledges support from The Swedish Foundation for International Cooperation in Research and Higher Education (STINT). We thank our referee for useful suggestions for improvements of the manuscript. This research has made use of the NASA/IPAC Extragalactic Database (NED) which is operated by the Jet Propulsion Laboratory, California Institute of Technology, under contract with the National Aeronautics and Space Administration.

## References

Adams, F.C., Lada, C.J., Shu, F.H., 1988, *ApJ* 326, 865

Belfort, P., Mochkovitch, R., Dennefeld, M., 1987, *A&A* 176, 1

Bergvall, N., 1985, *A&A* 146, 269

Bergvall, N., Olofsson, K., 1986, *A&AS* 64, 469

Bergvall N., Östlin G., Pharasyn A., Rönnback J., Masegosa J.: 1998, in *Highlights of Astronomy*, vol. 11

Bergvall, N., Östlin, G., 1999a, in preparation

Bergvall, N., Jörsäter, S., Martin, J.M., Östlin, G., 1999b, in preparation

Bergvall, N., Olofsson, K., 1999, in preparation

Burstein D., Heiles C., 1982, *AJ* 87, 1105

Boulanger, F., Prevot, M.L., Gry, C., 1994, *A&A* 284, 956

Carra, P., Hollenbach, D.J., Lord, S.D., Colgan, S.W.J., Haas, M.R., Rubin, R.H., Erickson, E.F., 1994, *ApJ* 423, 223

Chini, R., Kruegel, E., Lemke, R., Ward-Thompson, D., 1995, *A&A* 295, 317

Clegg, P.E., et al., 1996, *A&A* 315, L38

Colbert, J.W., Malkan, M. A., Clegg, P.E., Cox, P., Fischer, J., Lord, S.D., Luhman, M., Satyapal, S., Smith, H.A., Spinoglio, L., Stacey, G., Unger, S.J., 1999, *ApJ*, in press

Crawford, M.K., Genzel, R., Townes, C.H., Watson, D.W., 1985, *ApJ* 291, 755

Desert, F.-X., Boulanger, F.; Puget, J. L, *A&A*, 237, 215

Devereux, N.A., Young, J.S., 1990, *ApJ*, 359, 42

Dultzin-Hacyan, D., Moles, M., Masegosa, J., 1988, *A&A* 206, 95

Dultzin-Hacyan, D., Masegosa, J., Moles, M., 1990, *A&A* 238, 29

Fischer, J., et al., 1996, *A&A* 315, L97

Freedman, W., et al., 1994, *Nat* 371, 757

Garman, L.E., Young, J.S., 1996, *A&A* 154, 8

Garnett, D.R., Skillman, E.D., Dufour, R.J., Peimbert, M., Torres-Peimbert, S., Terlevich, R., Terlevich, E., Shields, G.A., 1995, *ApJ* 443, 64

Gerin, M., Phillips, T.G., 1998, *ApJ* 509, L17

Hawarden, T.G., Mountain, C.M., Leggett, S.K., Puxley, P.J., 1986, *MNRAS* 221, p41

Heisler, C.A., Vader, J.P., 1995, *AJ* 110, 87

Helou, G., Khan, I.R., Malek, L., Bohemer, L., 1988, *ApJS* 68, 151

Hildebrand, R.H., 1983, *QJRAS* 24, 267

Hollenbach, D., Tielens, A.G.G.M., Takahashi, T., 1991, *ApJ* 377, 192

Israel, F.P., Maloney, P.R., Geis, N., Herrmann, F., Madden, S.C., Poglitsch, A., Stacey, G.J., 1996, *ApJ* 465, 738

Jörsäter, S., Bergvall, N., 1999, in preparation

Kaufman, M.J., Wolfire M.G., Hollenbach, D.J., Luhman, M.L., 1999, *astroph/9907255*, submitted to *ApJ*. Also available at <http://dustem.astro.umd.edu>

Kennicutt R.C., 1989, *ApJ* 344, 685

Kennicutt et al., 1998, *ApJ* 498, 181

Kessler, M.F., et al., 1996, *A&A*, 315, L27

Krismer, M., Tully, R.B., Gioia, I.M., 1995, *AJ* 110, 1584

Lisenfeld, U., Ferrara, A., 1998, *ApJ* 496, 145

Loeb, A., 1993, *ApJ*, 404, L37

Lord, S., et al., 1996, *A&A* 315, 117

Lonsdale, C.J., Helou, G., 1985, 'Catalogued galaxies and quasars observed in the IRAS survey', Pasadena: JPL

Luhman, M.L., Satyapal, S., Fischer, J., Wolfire, M.G., Cox, P., Lord, S.D., Smith, H.A., Stacey, G.J., Unger, S.J., 1998, *ApJ* 504, L11

Madden, S.C., Poglitsch, A., Geis, N., Stacey, G.J., Townes, C.H., 1997, *ApJ* 483, 200

Malhotra, S., Helou, G., Stacey, G., Hollenbach, D., Lord, S., Beichman, C.A., Dinerstein, H., Hunter, D.A., Lo, K.Y., Lu, N.Y., Rubin, R.H., Silbermann, N., Thronson, H. A., Jr., Werner, M. W., 1997, *ApJ* 491, L27

Makarova, L.N., Karachentsev, I.D., 1998, *Astron. A&AS* 133, 181

Malkan, M.A., Gorjian, V., Tam, R., 1998, *ApJS* 17, 25

Maloney, P., Black J.H., 1988, *ApJ* 325, 389

Mochizuki, Kenji, Nakagawa, Takao, Doi, Yasuo, Yui, Yukari Y., Okuda, Haruyuki, Shibai, Hiroshi, Yui, Masao, Nishimura, Tetsuo, Low, Frank J., 1994, *ApJ* 430, L37

Östlin, G., Amram, P., Masegosa, J., Bergvall, N., Boulesteix, J., 1999a, *A&AS* 137, 419

Östlin, G., Amram, P., Bergvall, N., Masegosa, J., Boulesteix, J., 1999b, *A&A*, in preparation

Papaderos, P., Izotov Y.I., Fricke K.J., Thuan, T.X., Guseva, N.G., 1998, *A&A* 338, 43

Petrosian, V., Bachall, V., Salpeter, E.E., 1969, *ApJ* 155, L57

Poglitsch, A., Krabbe, A., Madden, S. C., Nikola, T., Geis, N., Johansson, L. E. B., Stacey, G. J.; Sternberg, A., 1995, *ApJ* 545, 293

Raymond J.C., 1979, *ApJS* 39, 1

Sandage, A., 1987, *AJ* 93, 610

Sanders, D.B., Scoville, N.Z., Soifer, B.T., 1991, *ApJ* 370, 158

Searle, L., Sargent, W.L.W., 1972, *ApJ* 173, 25

Skillman E.D., 1989, *ApJ* 347, 883

Smith, B.J., Madden, S.C., 1997, *AJ* 114, 138

Stacey, G.J., Geis, N., Genzel, R., Lugten, J.B., Poglitsch, A., Sternberg, A., Townes, C.H., 1991, *ApJ* 373, 423

Stark, A.A., 1997, *ApJ* 481, 587

Stasińska, G., 1982, *A&AS* 48, 299

Stasińska, G., 1990, *A&AS* 83, 501

Taniguchi, Y., Hamabe, M., Ichikawa, S., Yamagata, T., Iye, M., 1990,  
A&A 233, 385

Taylor, C.L., Kobulnicky, H.A., Skillman, E.D., 1998, AJ 116, 2746

Tielens, A.G.G.M., Hollenbach, D., 1985, ApJ 291, 722

Tonry, J.L., Blakeslee, J.P., Ajhar, E.A., Dressler, A., 1997, ApJ 475,  
399

Turner et al., 1998, ApJ 505, 207

Vila-Costas, M.B., Edmunds, M.G., 1993, MNRAS 265, 199

Watson, W.D., 1972a, ApJ 176, 103

Watson, W.D., Genzel, R., Townes, C.H., Werner, M.W., Storey,  
J.W.V., 1984, ApJL 279, L1 1972b, ApJ 176, 103

Wolfire, M.G., Tielens, A.G.G.M., Hollenbach, D., 1990, ApJ 358,  
116